Insufficient liver maturation affects murine early postnatal hair cycle

Toru Suzuki [a, *], Chisato Kikuguchi [a], Saori Nishijima [b], Tadashi Yamamoto [a, b, **]

[a] *Laboratory for Immunogenetics, Center for Integrative Medical Sciences, RIKEN, 1-7-22, Suehiro-cho, Yokohama, 230-0045, Japan*
[b] *Cell Signal Unit, Okinawa Institute of Science and Technology, 1919-1 Onna-son, Kunigami-gun, Okinawa, 904-0495, Japan*

ARTICLE INFO

ABSTRACT

Abnormal hair loss results from a variety of factors, such as metabolic dysfunctions, immunodeficiency, and environmental stressors. Here, we report that mutant mice having defects in liver function, develop alopecia. We have shown previously that in mice lacking a *Cnot3* gene, which encodes an essential component of the CCR4-NOT deadenylase complex in liver (*Cnot3*-LKO mice), the liver does not mature properly, resulting in various pathologies such as hepatitis, hepatic necrosis, and anemia. Unexpectedly, *Cnot3*-LKO mice start to lose hair around postnatal day 17 (P17). The region of hair loss expands all across their backs and symptoms persist until around P28-30. Afterward, hair re-grows, and *Cnot3*-LKO mice show complete hair recovery by P40. The phenotype is dependent on mouse genotype, indicating that hair follicle morphogenesis and cycling are influenced by abnormal liver development. By performing histological, quantitative PCR, and immunoblot analyses, we detected sebaceous gland (SG) hypertrophy accompanied by an increase of peroxisome proliferator-activated receptor γ (PPARγ). Collectively, these findings suggest that paracrine signaling related to liver function influences hair growth, at least in part, by altering lipid metabolism.

1. Introduction

Hair has many functions, including regulation of body temperature, protection of skin from sun and foreign objects, and dispersion of sweat-gland products [1]. It is highly desirable to develop therapeutics for hair loss or excessive hair growth, given the variety of hair growth disorders [1,2]. While mutations in keratins and other structural proteins are relevant to congenital hair defects, acquired hair loss or excessive hair growth generally result from aberrant hair follicle cycling [1,3]. Various factors such as inflammatory diseases, anemia, nutritional deficiencies, and drug treatments influence hair follicle cycling.

Hair follicles undergo repetitive growth and resting states. Hair cycling in mammals consists of three major stages, hair follicle growth (anagen), regression (catagen), and quiescence (telogen) [4,5]. Many rodents show synchronous follicular cycling [[4,5]]. Coupled with hair growth defects, this synchrony results in extensive hair loss, such as alopecia. Abnormal hair loss in mutant mouse strains offers novel insights into regulation of hair follicle morphogenesis and cycling, and further reveals the pathogenesis of alopecia in humans.

Iron deficiency anemia is relevant to the development of alopecia in humans [[6]]. A mouse model having a mutation in the transmembrane serine protease 6 gene developed alopecia associated with iron-deficiency anemia, indicating the importance of iron regulation for hair growth in various species [[7]]. Several studies report that lipid metabolism influences hair growth [[8]]. Targeted disruption of PPARγ in mouse hair follicle stem cells caused cicatricial alopecia, accompanied by altered lipid metabolism [9]. Insulin induced genes 1 and 2 (Insig 1/2) and glycerol kinase 5 (GK5) negatively regulate cholesterol biosynthesis. *Gk5*-deficient or epidermal specific *Insig*-deficient mice with excess cholesterol exhibited defects in hair growth [10,11]. Maternal factors also influence hair morphogenesis and growth. Pups developed alopecia if nursed by females lacking the *Pparγ* gene in hematopoietic and endothelial cells or by *Interleukin-10*-deficient (*Il-10*$^{-/-}$) females [12,13]. While *Pparγ*-deficiency led to production of inflammatory milk, affecting hair growth of nursing neonates [12], mast cell activation and iron deficiency contribute to hair loss in pups from *Il-10*$^{-/-}$ mother mice [13].

The CCR4-NOT complex triggers mRNA decay by shortening poly(A) tails [14–16]. Removal of unnecessary mRNAs by the CCR4-

NOT complex-mediated degradation exerts crucial regulatory control in biological processes [15—17]. We generated liver-specific *Cnot3* knockout mice (*Cnot3*-LKO mice) and found that postnatal liver functional maturation requires decay of mRNAs that are highly expressed in fetal and neonatal liver [18]. Here, we report the discovery of postnatal alopecia in *Cnot3*-LKO mice, revealing an unexpected relationship between liver development and hair growth.

2. Materials and methods

2.1. Mouse strain

Mice carrying the floxed allele of *Cnot3* (*Cnot3$^{flox/flox}$*) crossed with *Albumin*-cre (*Alb*-cre) and mTmG (Jackson Laboratory, #003574 and #007676, respectively) (*Cnot3*-LKO mice) have been described previously [18]. Genotypes were determined by PCR for the *Cnot3*-floxed allele, and the *Alb*-cre and mTmG transgenes. In this study, mice possessing genotypes of *Cnot3$^{+/+}$*, *Cnot3$^{flox/+}$*, *Cnot3$^{flox/flox}$*, *Cnot3$^{+/+}$:Alb*-cre, or *Cnot3$^{flox/+}$:Alb*-cre were considered controls. Mice were fed with CE-2 (Japan Clea). Experiments were performed according to animal use guidelines issued by the Committee of Animal Experiments at Okinawa Institute of Science and Technology Graduate University and the Institutional Animal Care and Use Committee of RIKEN, Yokohama Branch.

2.2. Tissue section

Skins were removed from euthanized mice and fixed with 10% formaldehyde overnight. Fixed skins were processed as paraffin-embedded sections (3 μm). Sections were stained with Hematoxylin 3G and Eosin (8656 and 8659, respectively, Sakura Finetek Japan) or toluidine blue (Sigma). Cryosections (6 μm) were employed for Oil Red-O (Merck) followed by Hematoxylin staining, or mTmG reporter protein detection, together stained with 4′,6-diamidino-2-phenylindole (DAPI, 1 μg/mL, Sigma, D9564). Images were captured using a BZ X-700 microscope (Keyence).

2.3. Quantitative real-time PCR (qPCR) analysis

Total RNA was extracted from dorsal skins using Isogen II, according to the manufacturer's protocol (Nippon Gene). RNA purity and concentration were evaluated by spectrophotometry using a NanoDrop ND-2000 (ThermoFisher). Total RNA (1 μg) was used for reverse transcription with oligo(dT)12-18primer (Invitrogen) using the SuperScript III First-Strand Synthesis System (Invitrogen). qPCR reactions were carried out with TB Green Premix Ex Taq (Takara) and a Viia 7 Sequence Detection System (Applied Biosystems). *Gapdh* mRNA levels were used for normalization. Relative mRNA expression was determined by the ΔΔCT method. Primers used in qPCR reactions are shown in Supplementary Table S1.

2.4. Immunoblotting

Tissues (liver or dorsal skin) were lysed with TNE lysis buffer (1% NP-40, 50 mM Tris—HCl [pH 7.5], 150 mM NaCl, 1 mM EDTA, 1 mM phenylmethylsulfonylfluoride, and 10 mM NaF). All antibodies were diluted at 1:1000 for incubation, except for PPARα (1:400 dilution). Immunoblot analysis was performed as described previously [19].

2.5. Antibodies

Anti-CNOT3 mouse monoclonal antibody was described previously [18]. Antibodies against GAPDH (#2118), PPARγ (#2443), C/EBPα (#8178), C/EBPβ (#3087), Cyclin D1 (#2978), and COX2 (#12282) were purchased from Cell Signaling Technology. Antibody against PPARα (42-4600) was from Thermo Fisher Scientific.

2.6. Statistical analysis

Statistical significance of differences between groups (control versus *Cnot3*-LKO) were tested using Student's t-tests (unpaired, two-tailed distribution with two-sample equal variance). We considered $P < 0.05$ as statistically significant.

3. Results

3.1. Cnot3-LKO mice lose back hair at early postnatal days

Hair growth usually started at P5-7 and showed normal progress until P14 in both control and *Cnot3*-LKO mice (Fig. 1A), although body size and liver histology differed between them [18]. When *Cnot3*-LKO mice reached P17-18, hair loss around their scapulae was observed. The area of hair loss gradually increased until it usually included their entire backs (Fig. 1A). Alopecia continued until P28-30. The hairless skin became pigmented, and hair re-appeared at P32-37. Around P48, hair of *Cnot3*-LKO mice became almost indistinguishable from that of control mice (Fig. 1A). Among littermates, control mice did not lose hair during this period (Fig. 1B). Even mice with genotype of *Cnot3$^{flox/+}$:Alb*-cre, which corresponds to *Cnot3*-heterozygous in liver, showed normal liver and dorsal hair histology. Hair loss phenotype was independent of genotype of parent mice, because *Cnot3*-LKO pups from various mating pairs lost hair, such as [*Cnot3$^{flox/+}$:Alb*-cre male and *Cnot3$^{flox/+}$* female], [*Cnot3$^{flox/+}$:Alb*-cre male and *Cnot3$^{flox/flox}$* female], [*Cnot3*-LKO male and *Cnot3$^{flox/+}$:Alb*-cre female], [*Cnot3$^{flox/+}$:Alb*-cre male and *Cnot3*-LKO female] and [*Cnot3*-LKO male and *Cnot3*-LKO female]. We performed immunoblot analysis and confirmed that CNOT3 is not suppressed in the skin of *Cnot3*-LKO mice (Fig. 1C), as we had already detected previously [18]. Furthermore, we used mice possessing an mTmG reporter transgene to examine whether Cre-mediated recombination is induced around skin. In the mTmG mouse strain, cells express green fluorescent protein (GFP) in response to Cre-mediated recombination; otherwise they express tdTomato [20]. We did not detect any cells expressing GFP in the skins of either control or *Cnot3*-LKO mice (Fig. 1D). These data strongly suggest that the hair loss phenotype was strictly dependent on liver abnormality caused by loss of CNOT3.

3.2. Hair loss in Cnot3-LKO mice is concomitant with follicular cyst formation and abnormal first postnatal catagen

We examined histology of affected skins during a period of several days. In control mouse skins, hair follicles were in late catagen and telogen from P20 to 24 (Fig. 2). The next anagen started from P24 to 28. The anagen stage proceeded as dermal papillae (DP) were well developed in the subcutis at P31 (Fig. 2). In contrast, hair follicles in the skin of *Cnot3*-LKO mice regressed in a manner different from normal catagen, with hypertrophy of SGs at P20 (Fig. 2). We confirmed the SG hypertrophy by staining lipids in sebocytes with oil red-O (Fig. 3A). Around P24, hair follicles formed cyst-like structures and some lost hair shafts. Abnormal catagen and telogen continued until about P28 (Fig. 2). We observed development of DP at P31 in the skins of *Cnot3*-LKO mice, as in control mouse skins, indicating that the first postnatal anagen had started [4]. The re-start of hair follicle cycling in *Cnot3*-LKO mice around P31 is consistent with pigmentation of skins at P35 (Fig. 1). These data suggested that the major defects occurred in the first postnatal catagen and telogen, promoted by abnormal liver function.
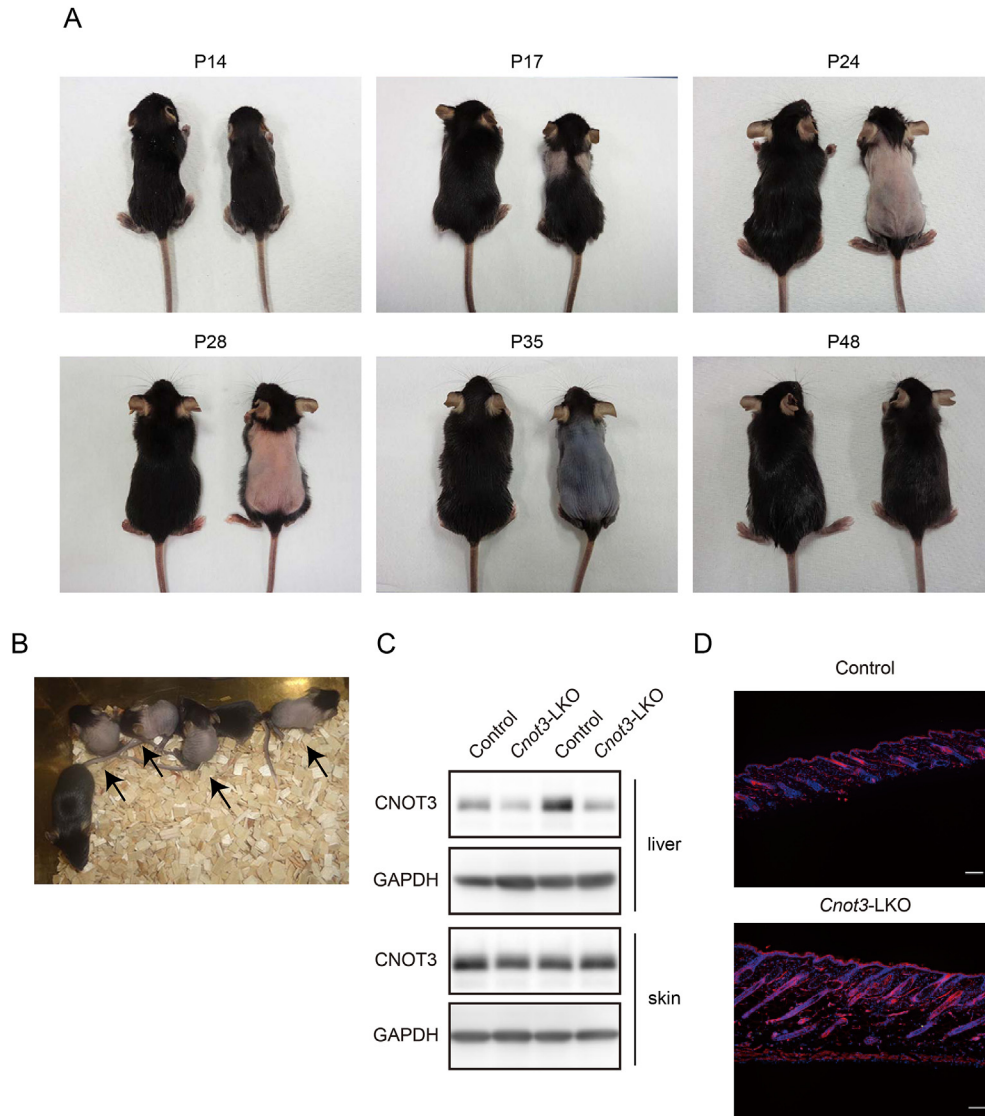
Fig. 1. *Cnot3*-LKO mice develop alopecia. (A) Comparison of hair growth at different times after birth in control (left) and *Cnot3*-LKO mice (right). (B) Specific hair loss in nursing *Cnot3*-LKO neonates (arrows) among littermates on P20. (C) Immunoblot of liver and skin lysates from control and *Cnot3*-LKO mice at P21. GAPDH was used as a loading control. (D) Frozen sections were prepared from dorsal skins of (+/+):*Alb*-cre/mTmG and *Cnot3*-LKO/mTmG mice at P21. The sections were stained with DAPI (blue) and analyzed to detect fluorescent proteins (red; tdTomato). Scale bars, 100 μm. (For interpretation of the references to colour in this figure legend, the reader is referred to the Web version of this article.)

3.3. Differential expression of mRNA and protein of the Ppar family in skins of Cnot3-LKO mice and controls

Several mouse models show postnatal hair loss phenotypes similar to those of *Cnot3*-LKO mice. Alopecia development in $Il10^{-/-}$ pups was associated with mast cell infiltration and degranulation in their skins [13]. Postnatal hair loss concomitant with aberrant follicular structure was relevant to inflammation in $Ppar\gamma^{flox/flox}$:-*Tie2*-cre mice [12]. The cyclooxygenase (COX)/prostaglandin pathway is one of the critical regulators of inflammatory responses, and importantly, overexpression of COX-2 in mouse skin led to alopecia [21,22]. We examined whether those conditions are responsible for hair loss in *Cnot3*-LKO mice. Toluidine blue staining revealed no significant difference in skins of control and *Cnot3*-LKO mice (Fig. 3B), indicating that mast cells are not responsible for alopecia in *Cnot3*-LKO mice. We performed qPCR analysis to compare expression of inflammatory genes in skins of control and *Cnot3*-LKO mice. *Il-1*, but not *Tnfα* mRNAs, increased significantly in skins of *Cnot3*-LKO mice (Fig. 4A). On the other hand, COX-2

actually decreased in skins of *Cnot3*-LKO mice (Fig. 4B). Therefore, inflammation seems unlikely to explain hair loss in skins of *Cnot3*-LKO mice. While Cyclin D1 is critical for stem cell differentiation in the outer root sheath [23], Cyclin D1 expression was comparable in skins of control and *Cnot3*-LKO mice. Because abnormal lipid accumulation was observed in SG, we next examined expression of *Pparα* and *Pparγ* mRNAs that encode transcriptional regulators critically involved in lipid metabolism. In addition, we examined expression of *Insig-2* and *Mpzl3* mRNAs, because a deficiency or mutation of those genes in mice resulted in hair growth abnormality [10,24]. Among mRNAs that we examined, *Pparα* mRNA decreased while *Pparγ* mRNA increased, both significantly, in skins of *Cnot3*-LKO mice (Fig. 4A). PPARγ protein consistently increased, although expression of PPARα protein did not completely reflect the results of qPCR (Fig. 4B). CCAAT/enhancer-binding protein (C/EBP)-α and -β are also important in regulation of adipocytes, and their robust expression in sebocytes indicates a role in differentiation and lipid metabolism of SGs [25]. Expression of C/EBP-α and -β was comparable in skins of control and *Cnot3*-LKO mice (Fig. 4B).
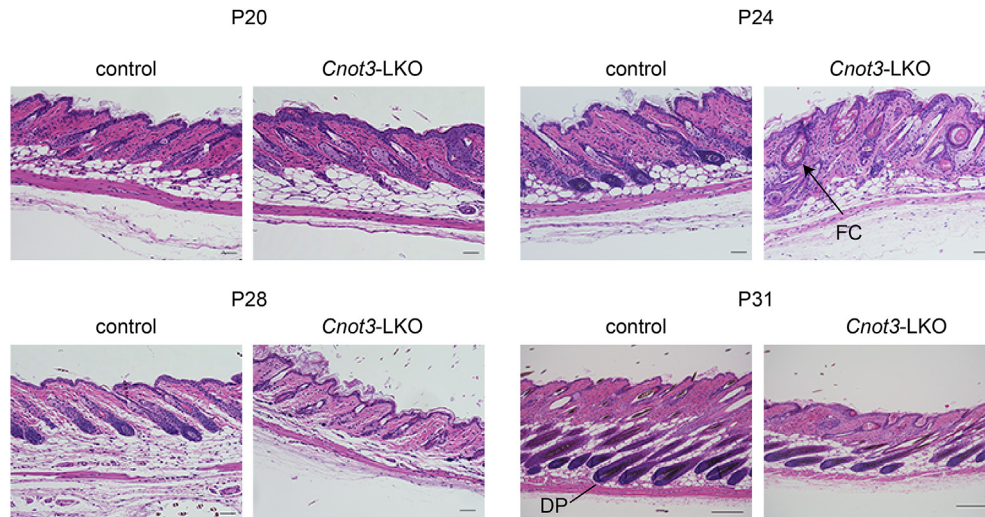
Fig. 2. Catagen and telogen in the dorsal skins of *Cnot3*-LKO mice exhibit abnormalities. HE-stained sagittal sections of dorsal skins in control and *Cnot3*-LKO mice at the indicated days of age. Scale bars, 50 μm (P20, 24, 28), 200 μm (P31).
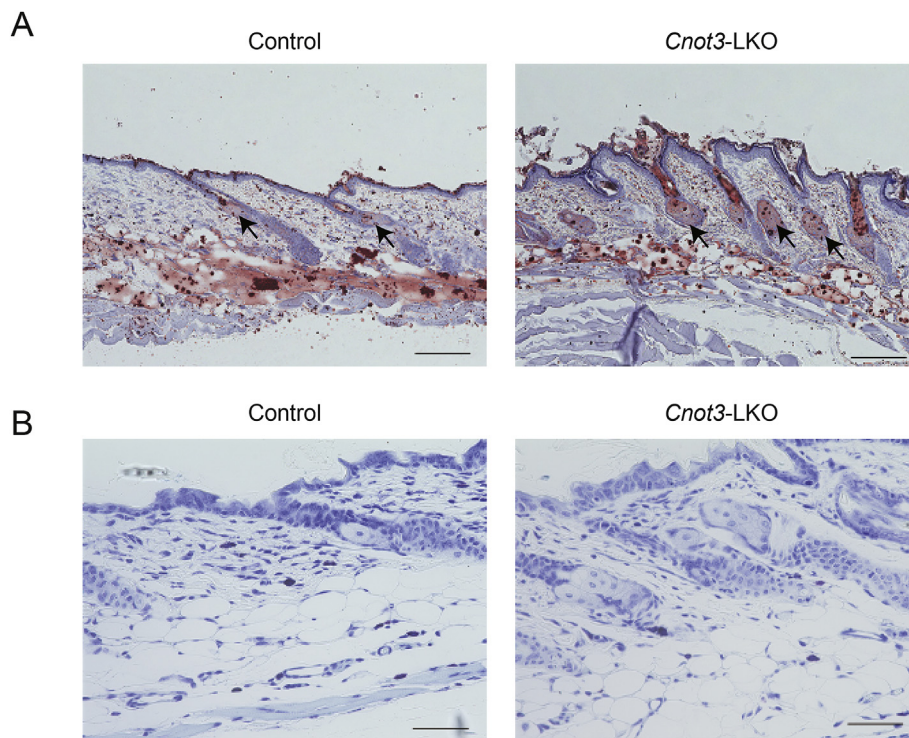

Fig. 3. Sebocyte hypertrophy in dorsal skins of *Cnot3*-LKO mice. (A, B) Oil red O-stained (A) and toluidine blue-stained (B) sagittal sections of dorsal skins in control and *Cnot3*-LKO mice at postnatal day 20. Scale bars, 100 μm (A), 50 μm (B). Arrow indicate sebocytes. FC and DP represent follicular-cysts and dermal papillae, respectively. (For interpretation of the references to colour in this figure legend, the reader is referred to the Web version of this article.)

Therefore, augmented expression of PPARγ is likely to influence SG function and neonatal hair cycle in skins of *Cnot3*-LKO mice.

4. Discussion

Extracellular molecules influence normal hair growth and cycling, as growth factors and growth factor receptors control hair follicle development and transitions between hair cycle stages [26]. Morphogens such as Sonic hedgehog and Wnt are also important [5]. When body fluids in the extracellular environment contain toxic molecules or lack essential nutrients, hair growth and maintenance are impaired through abnormal or ectopic signaling. In this study, we found that *Cnot3*-LKO mice developed alopecia. Livers of *Cnot3*-LKO mice did not develop mature functions due to an accumulation of unnecessary mRNAs and an insufficiency of mature liver-related mRNAs [18]. Because liver metabolizes many molecules, it is possible that liver abnormalities result in metabolite levels that are unfavorable for hair growth.

Timing of the appearance of alopecia in *Cnot3*-LKO mice was similar in pups of *PPARγ*$^{flox/flox}$;*Tie2*-cre or *Il-10*$^{-/-}$ mothers [12,13].
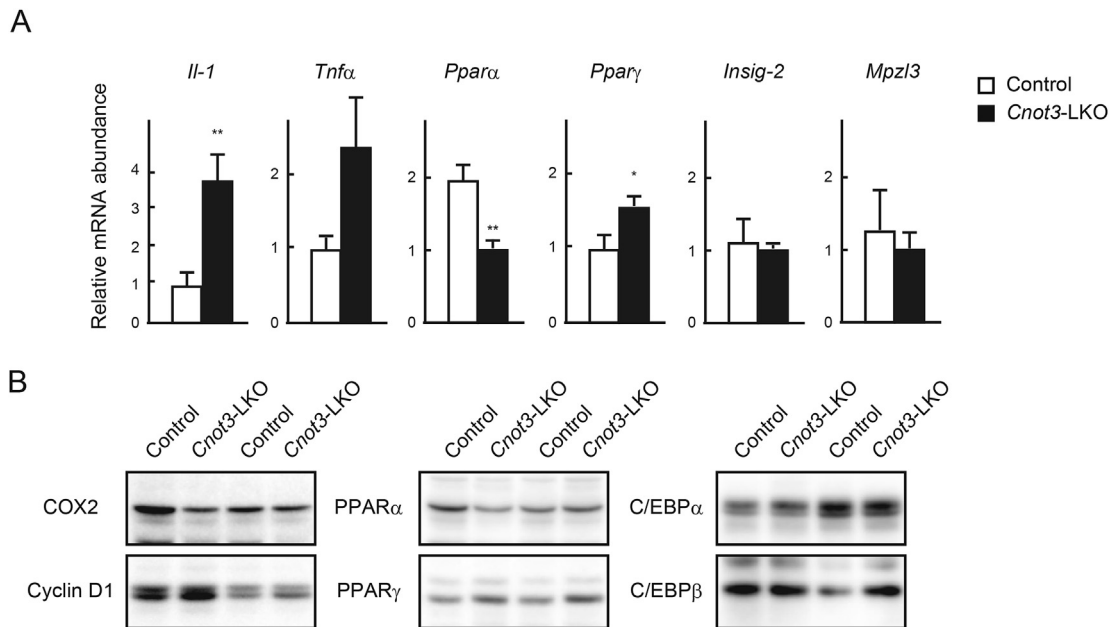
A

B

Fig. 4. Expression of genes related to inflammation and lipid metabolism differs in skins of control and *Cnot3*-LKO mice. (A) qPCR analysis of mRNAs in skins from P21 control and *Cnot3*-LKO mice (n = 6). *Gapdh* mRNA levels were used for normalization. Graphs show relative mRNA abundances of indicated genes. Data are mean ± standard error of the mean. *P < 0.05; **P < 0.01. (B) Immunoblot of skin lysates from P21 control and *Cnot3*-LKO mice. Lanes 1 and 2, and lanes 3 and 4 are littermates. See GAPDH blots in Fig. 1C, as the same lysates were used.

Furthermore, all mouse strains showed regrowth and subsequent complete recovery of hair. While maternal effects clearly explain hair recovery after pups of PPARγ$^{flox/flox}$:*Tie2*-cre or *Il-10*$^{-/-}$ mothers [12,13] are weaned, reasons for hair loss in young *Cnot3*-LKO mice remain to be addressed. Maternal effects hardly contribute to the hair loss, because littermates with wild-type genotype never lose hair (Fig. 1B). Iron-deficiency is one of the major reasons for alopecia in both humans and mice [6,7, 13]. The alopecia in pups of PPARγ$^{flox/flox}$:*Tie2*-cre was mainly due to increased inflammatory signaling [12]. *Cnot3*-LKO mice displayed both iron-deficiency anemia and hepatitis [18]. However, those pathologies persisted, and were exacerbated after weaning [18], suggesting that neither iron-deficiency nor inflammation is the primary cause of alopecia. On the other hand, we observed hypertrophy of SGs. Dysregulated SG functions are relevant to skin and hair diseases. SG atrophy was observed in human psoriatic alopecia and in a mouse model for primary cicatricial alopecia [27,28]. Moreover, rough coat mutant mice exhibited both SG hyperplasia and hair abnormalities [24]. Sebocytes in SGs produce and secret sebum, a lipid mixture. Impaired SG function reflected irregular cholesterol content in the skin, leading to hair loss [9–11]. We detected expression differences of *Ppar* family genes in the skins of control and *Cnot3*-LKO mice, suggesting developmental and functional change in SGs. Importantly, we observed lipid accumulation in neonatal liver and higher cholesterol content in the serum of *Cnot3*-LKO mice [18]. Whether those abnormalities affect SG function and hair growth remains to be determined.

In conclusion, postnatal liver development is responsible for hair follicle morphogenesis and cycling. Dysregulated liver function results in production of toxic molecules or nutrient deficiencies. Our findings show that liver abnormalities affect hair growth in a paracrine manner, contributing to the etiology of alopecia.

Author contributions

TS and TY conceived and designed the study and wrote the manuscript. TS performed the experiments. CK and SN maintained mouse strains and prepared samples for analyses.

Appendix A. Supplementary data

Supplementary data to this article can be found online at https://doi.org/10.1016/j.bbrc.2019.10.099.

Transparency document

Transparency document related to this article can be found online at https://doi.org/10.1016/j.bbrc.2019.10.099

References

[1] R. Paus, G. Cotsarelis, The biology of hair follicles, N. Engl. J. Med. 341 (1999) 491–497.
[2] D. Liyanage, R. Sinclair, Telogen effluvium, Cosmetics 3 (2016), https://doi.org/10.3390/cosmetics3020013.
[3] R. Paus, S. Muller-Rover, C. van der Veen, M. Maurer, S. Eichmüller, G. Ling, U. Hofmann, K. Foitzik, L. Mecklenburg, B. Handjiski, A comprehensive guide for the recognition and classification of distinct stages of hair follicle morphogenesis, J. Investig. Dermatol. 113 (1999) 523–532.
[4] S. Muller-Rover, B. Handjiski, C. van der Veen, S. Eichmuller, K. Foitzik, I.A. McKay, K.S. Stenn, R. Paus, A comprehensive guide for the accurate classification of murine hair follicles in distinct hair cycle stages, J. Investig. Dermatol. 117 (2001) 3–15.
[5] C. Blanpain, E. Fuchs, Epidermal stem cells of the skin, Annu. Rev. Cell Dev. Biol. 22 (2006) 339–373.
[6] L.B. Trost, W.F. Bergfield, E. Calogeras, The diagnosis and treatment of iron deficiency and its potential relationship to hair loss, J. Am. Acad. Dermatol. 54 (2006) 824–844.

[7] X. Du, E. She E, T. Gelbart, J. Truksa, P. Lee, Y. Xia, K. Khovananth, S. Mudd S, N. Mann, E.M. Moresco, E. Beutler E, B. Beutler, The serine protease TMPRSS6 is required to sense iron deficiency, Science 320 (2008) 1088–1092.

[8] K.S. Stenn, P. Karnik, Lipid to the top of hair biology, J. Investig. Dermatol. 130 (2010) 1205–1207.

[9] P. Karnik, Z. Tekeste, T.S. McCormick, A.C. Gilliam, V.H. Price, K.D. Cooper, P. Mirmirani, Hair follicle stem cell-specific *PPARγ* deletion causes scarring alopecia, J. Investig. Dermatol. 129 (2009) 1243–1257.

[10] B.M. Evers, M.S. Farooqi, J.M. Shelton, J.A. Richardson, J.L. Goldstein, M.S. Brown, G. Liang, Hair growth defects in Insig-deficient mice caused by cholesterol precursor accumulation and reversed by simvastatin, J. Investig. Dermatol. 130 (2010) 1237–1248.

[11] D. Zhang, W. Tomisato, L. Su, L. Sun, J.H. Choi, Z. Zhang, K. Wang, X. Zhan, M. Choi, X. Li, M. Tang, J.M. Castro-Perez, S. Hildebrand, A.R. Murray, E.M.Y. Moresco, B. Beutler, Skin-specific regulation of SREBP processing and lipid biosynthesis by glycerol kinase 5, Proc. Natl. Acad. Sci. U.S.A. 114 (2017), https://doi.org/10.1073/pnas.1705312114.

[12] Y. Wan, A. Saghatelian, L.-W. Chong, C.-L. Zhang, B.F. Cravatt, R.M. Evans, Maternal PPARγ protects nursing neonates by suppressing the production of inflammatory milk, Genes Dev. 21 (2007) 1895–1908.

[13] D.A. Vanderford, P.K. Greer, J.M. Sharp, M. Chichlowski, D.C. Rouse, M.A. Selim, L.P. Hale, Alopecia in IL-10-deficient mouse pups is c-Kit-dependent and can be triggered by iron deficiency, Exp. Dermatol. 19 (2010) 518–526.

[14] N.L. Garneau, J. Wilusz, C.J. Wilusz, The highways and byways of mRNA decay, Nat. Rev. Mol. Cell Biol. 8 (2007) 113–126.

[15] M.A. Collart, O.O. Panasenko, The Ccr4-Not complex, Gene 492 (2012) 42–53.

[16] R. Doidge, S. Mittal, A. Aslam, G.S. Winkler, Deadenylation of cytoplasmic mRNA by the mammalian Ccr4–Not complex, Biochem. Soc. Trans. 40 (2012) 896–901.

[17] Y. Shirai, T. Suzuki, M. Morita, A. Takahashi, T. Yamamoto, Multifunctional roles of the mammalian CCR4-NOT complex in physiological phenomena, Front. Genet. 286 (2014), https://doi.org/10.3389/fgene.2014.00286.

[18] T. Suzuki, C. Kikuguchi, S. Nishijima, T. Nagashima, A. Takahashi, M. Okada, T. Yamamoto, Postnatal liver functional maturation requires Cnot complex-mediated decay of mRNAs encoding cell cycle and immature liver genes, Development 146 (2019), https://doi.org/10.1242/dev.168146.

[19] T. Suzuki, J. Tsuzuku, R. Ajima, T. Nakamura, Y. Yoshida, T. Yamamoto, Phosphorylation of three regulatory serines of Tob by Erk1 and Erk2 is required for Ras-mediated cell proliferation and transformation, Genes Dev. 16 (2002) 1357–1370.

[20] M.D. Muzumdar, B. Tasic, K. Miyamichi, L. Li, L. Luo, A global double-fluorescent Cre reporter mouse, Genesis 45 (2007) 593–605.

[21] D.K. Bol, R.B. Rowley, C.P. Ho, B. Pilz, J. Dell, M. Swerdel, K. Kiguchi, S. Muga, R. Klein, S.M. Fischer, Cyclooxygenase-2 overexpression in the skin of transgenic mice results in suppression of tumor development, Cancer Res. 62 (2002) 2516–2521.

[22] K. Muller-Decker, C. Leder, M. Neumann, G. Neufang, C. Bayerl, J. Schweizer, F. Marks, G. Furstenberger, Expression of cyclooxygenase isozymes during morphogenesis and cycling of pelage hair follicles in mouse skin: precocious onset of the first catagen phase and alopecia upon cyclooxygenase-2 overexpression, J. Investig. Dermatol. 121 (2003) 661–668.

[23] X. Xu, S. Lyle, Y. Liu, B. Solky, G. Cotsarelis, Differential expression of cyclin D1 in the human hair follicle, Am. J. Pathol. 163 (2003) 969–978.

[24] T. Cao, P. Racz, K.M. Szauter, G. Groma, G.Y. Nakamatsu, B. Fogelgren, E. Pankotai, Q.-P. He, K. Csiszar, Mutation in *Mpzl3*, a gene encoding a predicted the adhesion protein, in the rough coat (rc) mice with severe skin and hair abnormalities, J. Investig. Dermatol. 127 (2007) 1375–1386.

[25] J.J. Bull, S. MuÈller-RoÈver, C.M.T. Chronnell, R. Paus, M.P. Philpott, I.A. McKay, Contrasting expression patterns of CCAAT/Enhancer-Binding protein transcription factors in the hair follicle and at different stages of the hair growth cycle, J. Investig. Dermatol. 118 (2002) 17–24.

[26] D. Peus, M.R. Pittelkow, Growth factors in hair organ development and the hair growth cycle, Dermatol. Clin. 14 (1996) 559–572.

[27] L. Rittié, T. Tejasvi, P.W. Harms, X. Xing, R.P. Nair, J.E. Gudjonsson, W.R. Swindell, J.T. Elder, Sebaceous gland atrophy is psoriasis: an explanation for psoriatic alopecia? J. Investig. Dermatol. 136 (2016) 1792–1800.

[28] M.R. Schneider, Fifty years of the asebia mouse: origins, insights and contemporary developments, Exp. Dermatol. 24 (2015) 340–341.